Transactions of The Indian Institute of Metals
Vol. 64, Issues 1 & 2, February-April 2011, pp. 81-84

Effect of copper and graphite addition on sinterability of iron

Felege Nekatibeb, A. Raja Annamalai and Anish Upadhyaya

Department of Materials Science & Engineering Indian Institute of Technology, Kanpur 208016, India

E-mail: felege123@gmail.com

Received 02 November 2010
Revised 31 January 2011
Accepted 03 February 2011
Online at www.springerlink.com

Keywords:
sintering; iron copper; copper steel.

Abstract

In ferrous powder metallurgy, copper and graphite are used as common alloying elements. Copper melts at low temperature compared to iron and forms liquid which promote interparticle bond formation. However, it also results in compact swelling. To negate this, graphite is used as an additive. This study examines the influence of copper and graphite addition on the densification, dimensional changes, and mechanical properties of iron compacts sintered at 1120°C. These properties have been correlated with the microstructure.

1. Introduction

Iron is highly ductile and soft metal. To improve its mechanical properties mostly alloying elements are added. Typical alloying elements include copper, nickel, carbon in the form of graphite, and phosphorus in the form of ferrophosphorus, Fe_3P. Among these copper and graphite are used as common alloying elements. Copper is added to increase strength, hardness and wear resistance of iron by forming substitutional solid solution and precipitation hardening, and for forming a liquid phase to activate sintering. During sintering copper melts at 1083°C below sintering temperature and forms liquid which rapidly distributes in the pore network of the compact from where it diffuses in to iron powders leaving large pores. Copper diffuses slowly into the iron particles and forms solid solution. The maximum amount of copper that can dissolve in gamma iron (austenite) is from 8 to 10 wt. %. In spite of improvement in mechanical properties copper addition causes pronounced swelling during sintering which is called copper growth. This phenomenon has been extensively investigated by different researchers [1-7]. Berner *et al*. [1] showed diffusion is too slow to account for the observed rapid rates of swelling. They suggested based on correlation between temperature dependence of swelling and the dihedral angle that expansion is due to penetration of the molten copper in space between the iron particles and into some grain boundaries inside the particles. Kayesser *et al*. [2] showed that flow of molten copper into interparticle contact areas and grain boundaries make greatest contribution in this swelling of Fe-Cu powder compacts. In similar manner carbon is added into iron to increase strength and hardness by forming pearlite microstructure. In addition to improvement in mechanical properties, for copper steels carbon has been used as a means of reducing the swelling induced by copper melt penetration. Jamil and Chadwick [4] and Lawcock and Davies [5] showed the dihedral angle between molten copper and iron increases with carbon content. Carbon segregation on grain boundaries lowers the interfacial energy between solid sold particles thereby increasing a dihedral angle. Thus the effect of graphite is to concentrate the copper at the grain corners by increasing dihedral angle. As dihedral angle increases, copper cannot penetrate and separate interparticle and/or interparticle grain boundaries therefore overall compact growth is restricted. Some of the most common alloy system in ferrous powder metallurgy are iron-copper, and copper steel. These alloys have been widely used for automotive applications. This is due to their lower cost of production, and in near net-shaping which satisfies close dimensional tolerance requirements for parts with complex geometries. This study examines the influence of copper and graphite addition on the densification, dimensional changes, and mechanical properties of iron in Fe-2Cu and Fe-2Cu-0.8Gr. alloys.

2. Experimental procedure

For present investigation, carbonyl Iron powder manufactured by Sigma-Aldrich, USA, Copper Powder (Atomized) manufactured by Metal Powder Company Ltd., India and Lorenz Graphite Powder (K5,15) manufactured by Lonza Ltd, Switzerland used as starting material. The as-received powder was characterized for apparent and tap density using set MPIF standards. The results are shown in Tables 1. The elemental Fe, Cu, and graphite powders were

Table 1 : Powder characteristics of Fe, Cu, and Graphite powders.

Characteristics		*Fe*	*Cu*	*Graphite*
Apparent Density, (g/cm^3)		2.6	4.58	0.17
Tap Density, (g/cm^3)		3.2	5.35	0.33
	D10	4.4	13.36	3.05
Particle size, μm	D50	10.24	28.39	7.6
	D90	28.39	57.35	16.8

weighted and mixed in a Turbula mixer (T2CNr.921266, Bachofen, AG, Germany) in to two different compositions (Fe-2Cu, Fe-2Cu-0.8Gr.) for half an hour. The mixed powders were compacted at 600MPa using a uniaxial semi-automatic hydraulic press (CTM 50, FIE, Ichalkaransi Maharastra, India) of 50 T capacity. The die made of high chromium high carbon steel was cleaned with acetone and was lubricated with zinc-stearate prior to each powder compaction to minimize friction. The sintering response on densification and microstructures were evaluated on to cylindrical pellets (16.08 mm diameter and 6 mm height). For measuring the tensile properties and transverse rupture strength, flat tensile bars and, transverse rupture test bars were pressed as per MPIF standards [10,11]. Sintering of the green (as-pressed) compacts were carried out in a MoSi2 heated at constant heating rate of 5°C/min in tubular furnace (OKAY 70T7, Bysakh & Co., India) that can attain maximum 1700°C under controlled atmosphere. To ensure uniform temperature distribution, during heating, intermittent isothermal hold for 15 min was provided at 540°C, 840°C. The sintered density was obtained by dimensional measurements and countercheked using Archimedes displacement method. For each condition, three samples were sintered and the average and the standard deviations were reported. The sintered density was expressed in grams per cubic centimetre and also normalized with respect to the theoretical density based on the weight fraction (w) of the respective component the theoretical density for a given composition (ρ^{th}) was calculated by inverse rule of mixture and is expressed as:

$$\frac{1}{\rho} = \sum_{i}^{n} \frac{w_i}{\rho_i} \qquad \text{(i)}$$

The extent of densification during sintering was also determined by calculating densification parameter. It is expressed as:

$$\text{Densification parameter} = \frac{(\text{s intered density - green density})}{(\text{theoretical density - green density})} \qquad \text{(ii)}$$

An optical microscope with digital image acquisition capability (LEICA DM2500, Leica Microsystems GmbH, and Germany) was used to obtain the micrographs of sintered samples. The samples were polished in a series of SiC emery papers (paper grades 220, 350, 500 and 1000), followed by cloth polishing using a suspension of 1 µm and 0.03 µm alumina diluted with water and the polished samples were etched with 3% Nital to determine the microstructures.

Micro hardness of the sintered samples was measured using Vickers Hardness Tester (model: V test, supplier: Bareiss, Germany with Load range 10 gm to 2 kg). Hardness measurements were taken on mirror finish polished sample by applying 0.05 kg of load for 10s. The lengths of the diagonals were measured using the software interface and an attachment integral with hardness tester. Tensile testing was carried out after each sample marked with 25.4 mm gauge length using universal testing machine (1195, INSTRON, UK) of capacity 10kN at a strain rate of $3.3\times10^{-4}s^{-1}$ (crosshead speed 0.5mm/min). The ultimate tensile strength and elongation of the tensile specimens were calculated after the test. To correlate the tensile properties with the microstructure, fractography analyses of the samples were carried out using SEM imaging (Zeiss Evo 50, Carl Zeiss SMT Ltd., UK). Dilatometric experiments were carried out with vertical type of dilatometer (UNITHERM^{TM} model 1161, Anter Corporation, PA, USA). The dimensional changes are periodically recorded throughout the sintering cycle as dilation (shrinkage/swelling) every 20 sec. allowing calculation of dilation rate. The compacts were heated using programmed sintering cycle at 5°C/min up to 1120°C isothermal sintering temperature for 30 min in a 90% N2 -10% H_2 atmosphere, then to cooled down at rate of 5°C/min to room temperature.

3. Results and discussions

3.1 Densification response

Table 2 compares the densification response of sintered Fe, Fe-2Cu, and Fe-2Cu-0.8Gr. compacts. Sintered densities achieved for all the sintered samples have no significant difference they are almost similar. This is due to low sintering temperature. Considering densification parameter for sintered samples, iron shows more densification due to higher shrinkage. Fe-2Cu has less densification. This indicates compact swelling due to copper growth phenomenon. In case of Fe-2Cu-0.8Gr. densification is more than Fe-2Cu one. This shows the role of carbon in improving densification response of the copper steel by restricting growth of copper.

Table 2 : Effect of heating mode on the densification of Fe, Fe-2Cu, and Fe-2Cu-0.8Gr. Compacts sintered at 1120°C with 30min soaking time.

Composition	*Green Density (ρs)*	*Sintered Density, g/cm^3*	*Sintered Density, % Theor.*	*Densification Parameter*
Fe	6.46±0.06	6.8±0.4	87.5±5.5	0.29±0.04
Fe2Cu	6.56±0.1	6.9±0.5	87.3±6.0	0.24±0.03
Fe2Cu0.8Gr	6.49±0.1	7.0±0.1	91.4±1.0	0.45±0.09

3.2 Microstructure evolution

Figures 1and 2 show optical and SEM microstructures of pure Fe, Fe-2Cu, and Fe-2Cu-0.8Gr compacts in as-sintered condition. It is clear from micrographs that compared to pure Fe, Fe-2Cu has more amount of pores with great size since Cu powder melts at 1083°C and liquid Cu spreads between the Fe particles and changes to thin liquid films which lead to swelling as a result the prior sites for the particles becomes void. As can been seen, in micrograph of Fe-2Cu in the iron matrix non homogeneously distributed copper concentrated regions are observed after sintering. This is because at room temperature solubility of copper in iron is around 0.4% which is very less as compared to initial amount, hence the excess copper precipitates out and the region of higher copper concentrations appears more brownish on the micrograph. The micrograph of Fe-2Cu-0.8Gr shows undissolved copper that is due to the addition of 0.8% graphite which hinders the flow of liquid Cu in Fe particles.

3.3 Mechanical properties

Table 3 shows the effect of alloying elements on the bulk hardness (HRB), strength, ductility, and transverse rupture strength (TRS) of Fe, Fe-2Cu, and Fe-2Cu-0.8Gr. sintered compacts. The bulk hardness increases from iron to copper steel. Tensile strength and TRS value of iron is improved on addition of copper and carbon. These results can be attributed to increased sinter bonding by liquid phase

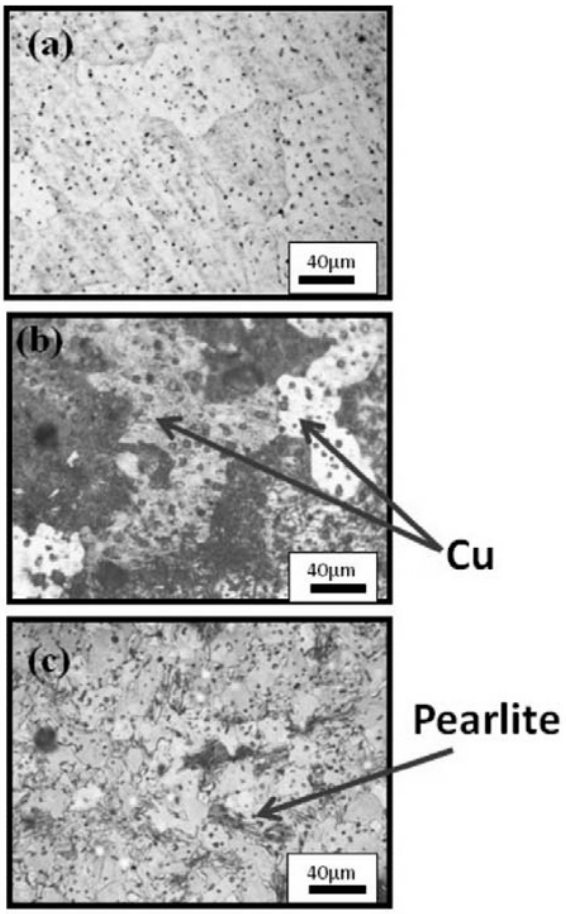

Fig. 1 : Etched optical microstructures of (a) pure Fe, (b) Fe-2Cu, and (c) Fe-2Cu-0.8Gr sintered at 1120°C for 30 min in a 90%N2 /10%H2atmosphere.

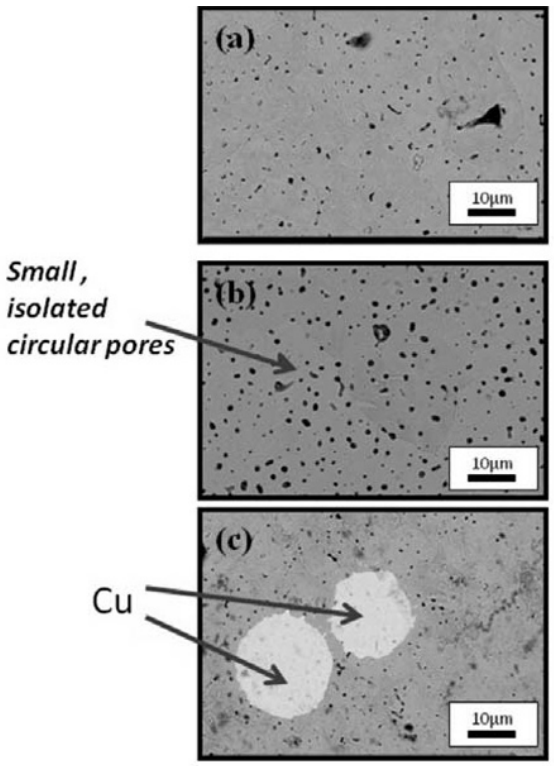

Fig. 2 : SEM microstructures of (a) pure Fe, (b) Fe-2Cu, and (c) Fe-2Cu-0.8Gr sintered at 1120°C for 30 min in a 90%N2 /10%H2atmosphere.

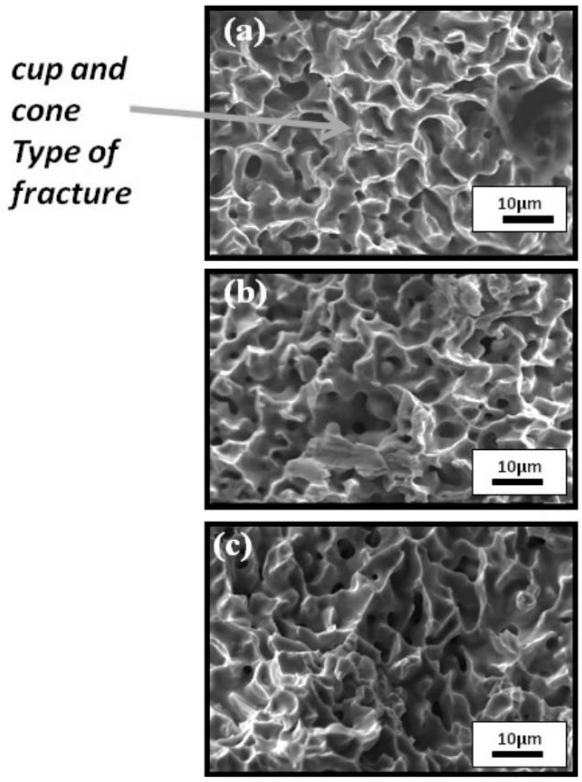

Fig. 3 : SEM fractographs of (a) pure Fe, (b) Fe-2Cu, and (c) Fe-2Cu-0.8Gr sintered at 1120°C for 30 min in a 90%N_2 /10%H_2 atmosphere.

Table 3 : Effect of heating mode on the mechanical properties of Fe, Fe-2Cu, and Fe-2Cu-0.8Gr. compacts sintered at 1120°C with 30min soaking time.

Composition	*Micro hardness, HV0.05*	*Strength, MPa*	*Elongation, %*	*TRS, MPa*
Fe	128± 6	125±19.4	10.4±0.1	371±67.7
Fe2Cu	179±7	183±31	1.5± 1.4	638±28
Fe2Cu0.8Gr	184±41	206±2.4	2.6 ±0.5	841±25.4

sintering, copper solid solution hardening and the formation of pearlite structure due to addition of carbon. Figure 4 shows SEM fractographs of the tensile samples. It is clear from these micrographs that all the sintered samples showed cup and cone type of fracture which is characteristics of ductile failure.

3.4 Dilatometric study

Figure 4 shows the dilatometric plot of both axial dilation (%), temperature(°C) and time (minutes) of Fe, Fe-2Cu, and Fe-2Cu-0.8Gr. compacts heated at 5°C/min to 1120°C for 30 min in a 10%H2/ 90%N_2 atmosphere. Pure iron curve comprises different events. The first event is ferrite to austenite transformations, which is observed as great depression on the plot around 910°C (A). The second event is phase transformation from austenite to ferrite(C). Iron copper (Fe-2Cu) undergone same situation as pure iron, in addition, it shows the copper melt phenomena which occurred at 1083°C (B) and it is indicated as a spike on the plot. Axial shrinkage of pure iron decreased as a result of copper growth phenomenon. Copper steel Fe-2Cu-0.8Gr also undergone same situation as pure iron and iron carbon. Furthermore, it shows the copper melt phenomena which occurred at 1083°C

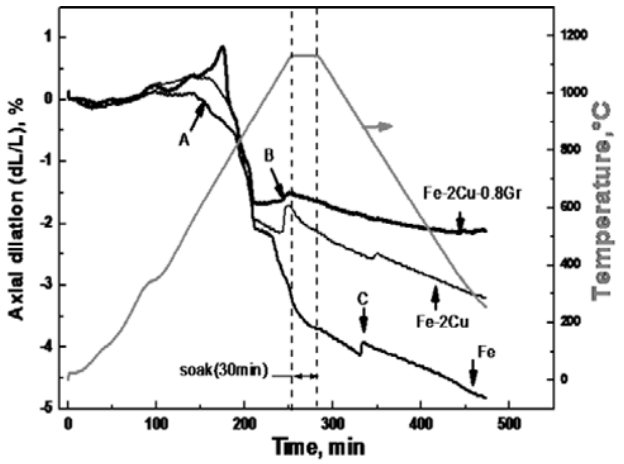

Fig. 4 : Dilatometric plot of axial dilation (%), temperature and time (minutes) of Fe, Fe-2Cu, and Fe-2Cu-0.8Gr. compacts heated at 5°C/min to 1120°C for 30 min in a 90%N2 /10%H2 atmosphere.

and it is indicated as a small spike on the plot. The large expansion associated with the Copper growth phenomenon which is observed on Fe-Cu curve decreased in this case. This is due to addition of 0.8 % graphite which increased the dihedral angle between iron and copper and hence wetting is inhibited.

4. Conclusions

Pure iron showed high shrinkage which promote better densification but increasing dimensional tolerance. Addition of copper resulted less shrinkage in iron due to copper melt penetration of iron particles and resulted better mechanical properties due to improved sinter bonding through liquid phase sintering. Carbon addition reduced copper growth and greatly improved mechanical properties by forming pearlit microstructure. Fractographs of the tensile bars showed that sintered samples undergone ductility fracture (cup and cone). SEM micrographs indicated small, isolated circular pores, which are the reason for improvement observed in mechanical properties by reducing stress concentration at pore site.

References

1. Berner D, Exner H and Petzow G, Swelling of Iron-Copper Mixtures during Sintering and Infiltration, *Modern Developments in Powder Metallurgy*, **6** (1973) 237.
2. Kaysser W, Huppmann W and Petzow G, Analysis of Dimensional Changes during Sintering of Fe-Cu, *Powder Metallurgy*, **23** (1980) 86.
3. Tabeshfar K and Chadwick G A, Dimensional Changes during Liquid Phase Sintering of Fe-Cu Compacts, *Powder Metallurgy*, **27** (1984) 19.
4. Jamil S and Chadwick G, Investigation and Analysis of Fe-Cu and Fe-Cu-C Compacts, *Powder Metallurgy*, **28** (1985) 65.
5. Lawcock R and Davies T, Effect of Carbon on Dimensional and Microstructural Characteristics of Fe-Cu Compacts during Sintering, *Powder Metallurgy*, **33** (1990) 147.
6. Wanibe Y and Yokoyama H. Itoh T, Expansion during Liquid Phase Sintering of Iron-Copper Compacts, *Powder Metallurgy*, **33**(1) (1990) 65.
7. Griffo A and German R M, Dimensional Control in the Sintering of Iron-Copper-Carbon via Particle Surface Area, *The International Journal of Powder metallurgy*, **30**(4) (1994) 399.
8. Kuroki H, Gang Han and Kenji Shinozaki, Solution-Repreicipitation mechanisms in Fe-Cu-C during liquid phase sintering, *The International Journal of Powder metallurgy*, **35**(2) (1999) 57.
9. Nayer A., *The Metals Data Book*, McGraw-Hill, New York, NY, (1997).
10. MPIF Standard 10: tension test specimens for pressed and sinter metal powders, Standardtest methods for Metal Powders and Powder Metallurgy Products, Metal Powder Industries Federation, Princeton, NJ, USA, (1991).
11. MPIF Standard 41: Determination of transverse rupture strength of sintered metal powder test specimen, Standard Test methods for Metal Powders and Powder Metallurgy Products, Metal Powder Industries Federation, Princeton, NJ, USA, (1991)
12. ASM Handbook, Powder Metal Technologies and Applications, *ASM International*(OH), **7** (1998)
13. German R M, *Powder Metallurgy of Iron and Steel*, J. Wiley & Sons Inc., New York, NY, USA, (1998).
14. Salak Andrej and Riecansky, *Ferrous Powder Metallurgy*, Cambridge International Science Publishing, (1995).